Experimental Study of the Internal Wave Damping on Small-Scale Turbulence

L. A. OSTROVSKY

Cooperative Institute for Research in Environmental Sciences, University of Colorado/NOAA Environmental Technology Laboratory, Boulder, Colorado

V. I. KAZAKOV, P. A. MATUSOV, AND D. V. ZABORSKIKH

Institute of Applied Physics of Russian Academy of Sciences, Nizhni Novgorod, Russia

14 March 1995 and 3 July 1995

ABSTRACT

The interaction between internal waves (IW) and small-scale turbulence is investigated in a laboratory tank with thermocline-type stratification. Turbulence has been produced by an oscillating grid. Temperature and velocity measurements have been provided. The turbulent energy distribution and the dependence of the IW damping rate on the wavenumber have been measured. The damping rates for IW, calculated based on a semiempirical model for turbulence, demonstrate a quantitative agreement with experimental data.

1. Introduction

The interaction between internal gravity waves (IW) and small-scale turbulence is one of the most important factors governing the dynamics of the upper ocean. There are different possible mechanisms of energy transfer from IW to turbulence. One of them is the breaking of IW with the formation of turbulent spots (e.g., see Woods 1968; Monin and Ozmidov 1985). Various estimates relevant to this kind of processes have been broadly discussed in the literature (e.g., see Monin and Ozmidov 1985). Weinstock (1987) has carried out computations for the case of atmospheric IW and demonstrated the effective generation of turbulence by the local velocity shear in IW. Such processes are associated with sufficiently strong IW having the local Richardson number small enough to provide their instability and breaking, which does not seem to be prevalent in the ocean.

This stimulated investigations of possible mechanisms of energy exchange between IW and turbulence without breaking. There exists some indirect evidence of the energy transfer from IW to turbulence in the ocean that is not caused by the IW breaking (e.g., see Gargett 1984). A considerable amplification of the turbulent energy by IW was demonstrated in a laboratory experiment by Matusov et al. (1989).

Corresponding author address: Dr. Lev A. Ostrovsky, U.S. Dept. of Commerce, NOAA/ERL/ETL, 325 Broadway, R/E/ET 1, Boulder, CO 80303-3328.
E-mail: ola@wpl.erl.gov

Another aspect of such phenomena is the damping of the IW due to the energy consumption by turbulence. LeBlond (1966) considered theoretically the IW damping due to the turbulent viscosity in a stratified fluid layer with a constant Brunt–Väisälä (buoyancy) frequency. Ostrovsky and Soustova (1979), Ivanov et al. (1983), and recently Ostrovsky and Zaborskikh (1996) developed a model of IW damping in the turbulent upper ocean with a thermocline and small-scale turbulence enhancement in the IW field based on the semiempirical theory of turbulence. It was shown there that, together with turbulent viscosity, the turbulent diffusion in the thermocline plays an important role and that the losses can be very significant even for long IW, up to the inertial range.

Experimental observations of the IW damping by turbulence were performed several times in laboratory experiments (see Phillips 1980; Kantha 1980; Barenblatt 1978). However, these results should have been regarded rather as qualitative demonstrations of the effect. No quantitative measurements or comparisons with theoretical models have been made. Moreover, most of the studies referred to the two-layer fluid or linear density profiles, which restricts the application of the results to the real ocean conditions where the seasonal thermocline may play a decisive role.

Here, we present the results of laboratory experiments on IW attenuation on small-scale turbulence, performed under conditions imitating those in the upper ocean: thermocline-type stratification and inhomogeneous vertical distribution of turbulence that is typically produced by wind stress and/or surface wave breaking. The experimental data are compared with

theoretical estimates based on the semiempirical theory of turbulence and show a quantitative agreement.

2. Experiment

Experiments on the IW attenuation in the turbulent region have been conducted in a thermostratified tank (see Arabadzhi et al. 1984) with dimensions 5.5 m × 1.6 m × 1.2 m (Fig. 1). Thermal stratification was provided by two pairs of heat exchangers (warm and cold). The temperature profile was similar to that observed in tropical seas, with pronounced thermocline and temperatures 20°–22°C in a 30-cm thick upper layer and 4°–8°C below the thermocline [$T(z)$ profile is sketched in Fig. 1]. The maximum buoyancy frequency was about 0.35–0.4 rad s^{-1}. Pronounced seasonal thermocline in the sea is usually located at depths of 20–40 m, which results in a spatial scaling factor of about 100 (or 10 for timescales and for velocities). The characteristic buoyancy period ranges from 2 to 5 min in oceanic conditions, which corresponds to those in the tank about 16–20 s, actually observed. Internal waves were generated by a wavemaker in the form of a semicircular cylinder with a diameter of 10 cm, oscillating with amplitude up to several centimeters about the central position which coincided with the location of maximum buoyancy frequency. This facility allowed us to cover the wavelength range from 10–20 cm up to 2 m by driving the wavemaker with periods of 20–50 s, for which the first IW mode was dominant. The measurements were performed in a channel 1.5 m long, 50 cm wide, and 1 m deep separated from the remaining volume of the tank by two parallel vertical Plexiglas plates placed at 70 cm from the wavemaker, as shown in Fig. 1. Such a configuration was chosen to enable the maintaining of turbulence in a relatively small region and thus avoid fast entrainment and mixing, which could change greatly the temperature profile and, hence, the efficiency of the wavemaker and dispersion characteristics for the IW. We checked the temperature profile before, during, and after each set of measurements, and found that the buoyancy period changes by less than 10%, which is in the limits of the accuracy of the experiment.

The turbulence was produced by an oscillating grid, which is a widely studied source of turbulence (e.g., see review by Britter 1983). The grid (perforated aluminum plate with dimensions 20 cm × 45 cm and mesh size about 3 cm) was placed at 6 cm below the water surface in the middle of the channel and driven with frequencies of 4–6 Hz and magnitudes of about 3–5 mm. Such regimes allowed us to experiment for four to six hours with no significant changes in thermocline.

The measurement facilities included

- a movable temperature probe, comprised of a thermistor with a low time constant, was used to obtain temperature profiles in the beginning and in the end of each experiment
- two copper temperature sensors (referred below as wire sensors) were constructed as 50-cm long probes with a time constant about 2 s. These sensors are sensitive to temperature variations caused mainly by IW of the first mode and practically insensitive to small-scale turbulent temperature fluctuations
- a hot-wire anemometer measured turbulent velocity fluctuations.

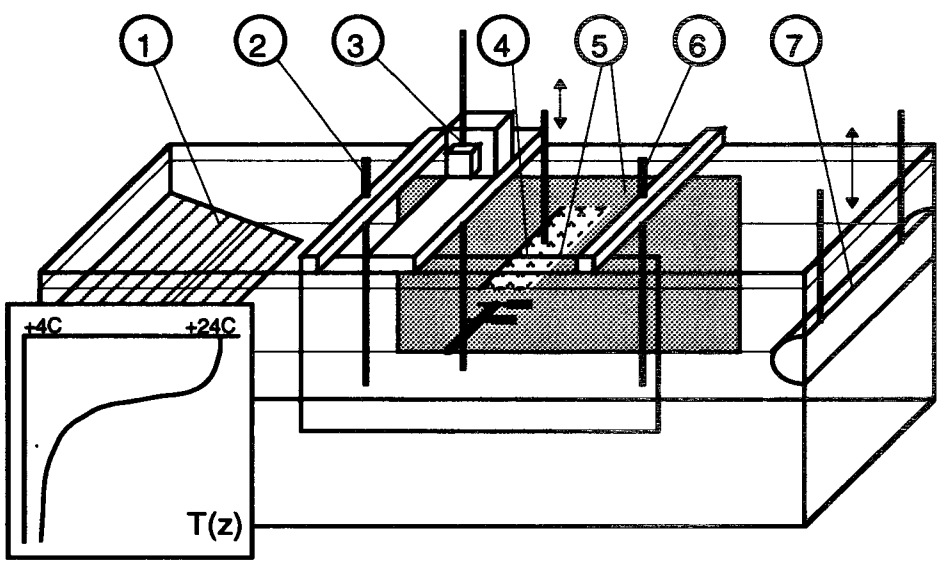

FIG. 1. Experimental setup: (1) IW absorber, (2) and (6) wire temperature sensors, (3) scanning tool with a thermistor and a hot-wire anemometer, (4) oscillating perforated grid, (5) vertical Plexiglas walls, and (7) wavemaker for IW.

The data were collected and processed using a Compaq 4/33 computer.

Figure 2 illustrates vertical distributions of buoyancy frequency N and characteristic profile of turbulent energy b calculated from the measurement data.[1] The profiles of the vertical component of velocity in the IW have been computed for the measured $N(z)$ profile and wavenumbers $k = 0.1$ and 0.6 of the first IW mode and also plotted in Fig. 2. Figure 3 represents the dispersion law for the first mode of IW in $\omega(k)$ and $\lambda(T)$ planes (λ and T are the wavelength and period of IW, respectively). The detailed measurements of turbulence have been made in the region from -30 to 30 cm in a horizontal direction with respect to a grid center and in the depth range from 1 to 30 cm with 5-cm spatial intervals both in horizontal and vertical directions. The velocity fluctuations were recorded, filtered with a high-frequency filter with a time constant of 20 s, and then processed to compute rms velocity fluctuations. These data are plotted in Fig. 4 in a topographic way, with curves representing the isolines of turbulent energy. The turbulence reaches its maximum at the grid and decays away from it both in vertical and horizontal directions.

Internal waves were measured by two wire sensors: the first placed at 70 cm from the wavemaker and 50 cm in front of the grid and the second at 50 cm behind the grid.

The effect of turbulence on continuously excited IW is illustrated Fig. 5. The plot represents two records of IW made by wire sensors. Upper and lower curves correspond to the first (50 cm upstream from the grid) and the second (50 cm downstream) sensors. The moments of switching the grid drive on and off are shown by dotted vertical lines. The gap in the records was needed for the IW decay after the first experiment. Switching on of the grid slightly affects the IW amplitude in front of the grid, but the wave passed through the region of turbulence decays much stronger.

These records were processed with an FFT algorithm using a 128-point running window. Power spectra of IW exhibited pronounced peaks at the wavemaker oscillation frequency, thus allowing us to measure only the amplitudes of the most intensive harmonic.

However, for the continuous regime this result must be considered only as a qualitative one. Actually, in the continuous regime the results are influenced considerably by reflection of IW from the terminal end of the tank. This amplitude can reach up to 20% of that of an initially excited wave. The phase of a reflected wave with respect to the excited one is not controlled, which can lead to the 20% error in IW amplitude and hence up to 80% error in values of A_1/A_0. Special measures to provide the absorption of IW at the terminal end reduced considerably (almost by half) the amplitude of the reflected wave, but this reduction was still insufficient to provide reliable enough measurements.

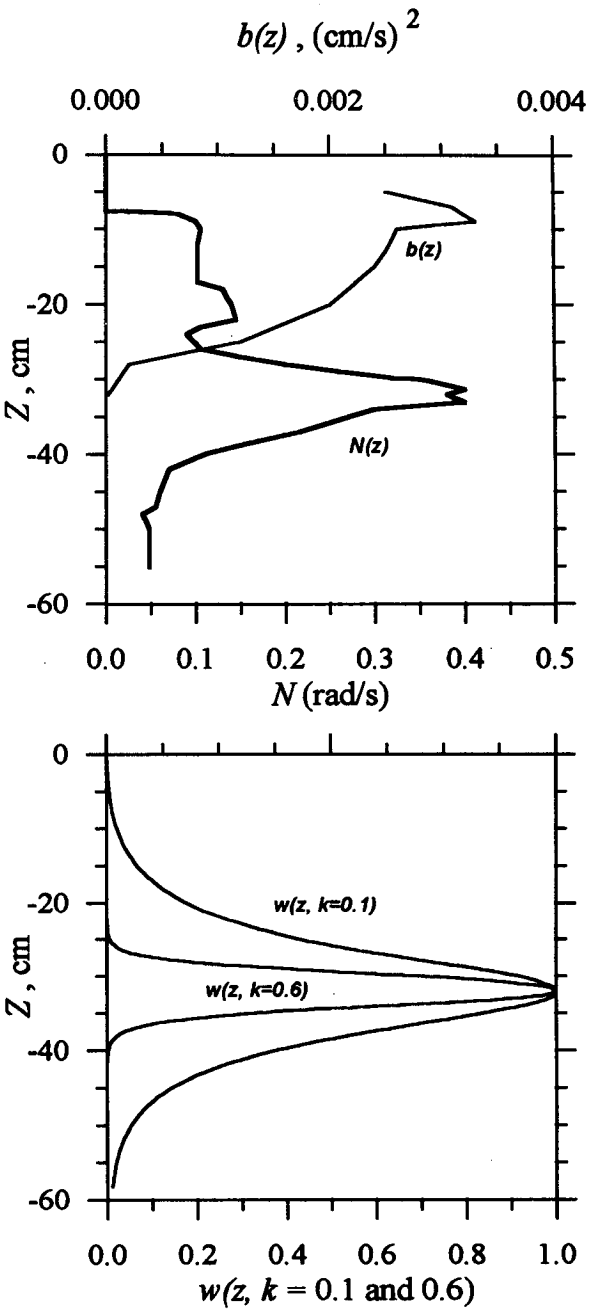

FIG. 2. Vertical distributions of turbulent energy $b(z)$, Brunt–Väisälä frequency $N(z)$, and the computed vertical velocity component w in the first IW mode; the latter is computed for $k = 0.1$ and $k = 0.6$.

[1] In this experiment we were able to measure only one turbulent velocity component, u', and the kinetic energy of turbulent motions was defined as $b = (3/2)\langle u'^2 \rangle$; that is, turbulence is regarded as isotropic, which is justified by its relatively small scale and by comparison with the theory given below.

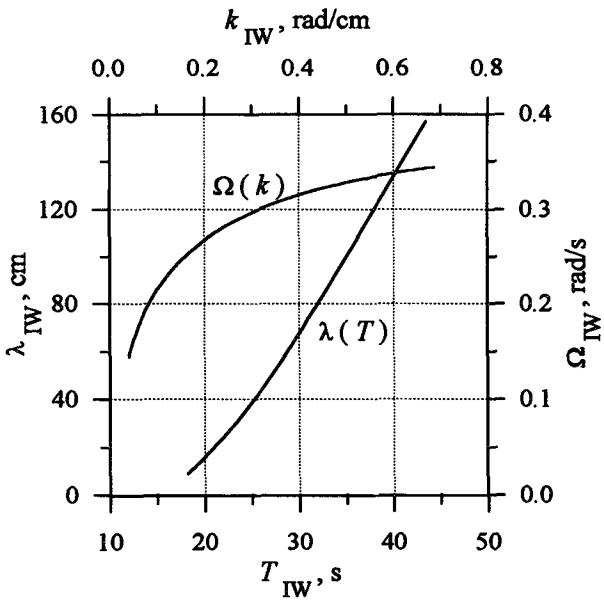

FIG. 3. Dispersion curves for the first IW mode in the tank: $\omega(k)$ and $\lambda(T)$.

To eliminate the errors caused by reflected waves, we used short wave trains instead of a continuous generation of IW. The results of the measurements are shown in Fig. 6. The upper plot represents the displacement of thermocline due to IW recorded by the first (A) and second (B) sensors, and the lower plot displays the temporal behavior of IW amplitudes. The wave trains were 10–15 periods long in our experiments. Here, FFT processing was performed inside of a running short 64-point flat-top window. Such a narrow window (only two minutes long) was chosen in order to decrease the transient time of amplitude averaging, although it led to slightly larger errors in amplitude.

Here, we again observe a considerable IW damping after traveling through the turbulent region. All results discussed below are obtained in experiments with the grid placed 6 cm below the surface and driven with a frequency of 5 Hz and peak-to-peak amplitude of about 5 mm. Such a configuration of the setup provided not only a turbulence level sufficient to effect the IW with no fast mixing but also greatly reduced the steady currents near the thermocline, which was verified by using dye tracers. The IW period ranged from 23 to 45 s, which corresponds to wavelengths of from 35 to 170 cm (wavenumber from 0.035 to 0.18 rad cm^{-1}). The data of 13 experiments are represented in Fig. 7 by squares. Vertical bars represent errors in IW amplitude measurements and horizontal bars, errors in wavenumber estimation due to uncertainty in IW period measurements (1.5 s). The A_1/A_0 ratio equal to unity corresponds to the absence the turbulence. In spite of the considerable scatter of experimental data, the trend of increasing IW decay in the turbulent region with the wavenumber growth is pronounced. The solid curve represents the theoretical estimate for the IW decay, which will be discussed below.

3. Theoretical estimates

A theoretical model for IW propagation in the turbulent stratified liquid is based on the well-known set of two-dimensional semiempirical equations including the dynamic equations of stratified fluid and the equation for turbulent energy (e.g., see Rodi 1987; Miropolsky 1981):

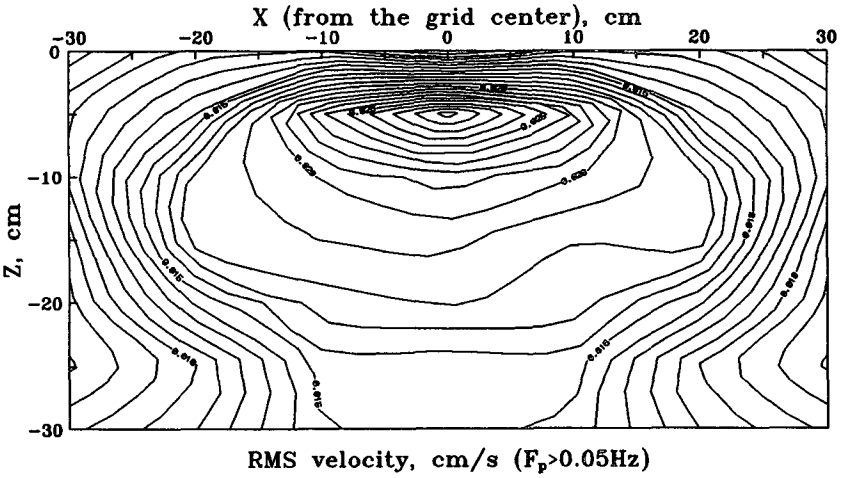

FIG. 4. Isolines of turbulent energy in the X–Z plane in the middle of the tank (velocity pulsations have been filtered with HF filter with 20-s cutoff period).

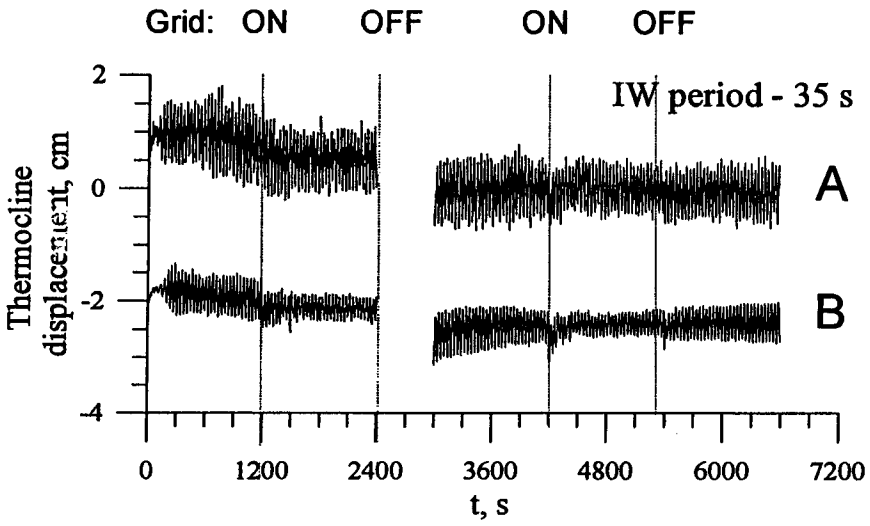

FIG. 5. Internal wave attenuation by turbulence: experiment with continuous generation of IW. The grid was located at 17 cm below the surface and driven with frequency 6 Hz and peak-to-peak amplitude 3 mm. The plot represents the records of temperature made at 50 cm before (A) and 50 cm after the grid (B). The moments of the grid switching on and off are shown.

$$\frac{\partial \mathbf{U}}{\partial t} + (\mathbf{U}\nabla)\mathbf{U} + \nabla\frac{p}{\rho_0} - \mathbf{g}\frac{\rho}{\rho_0} = \frac{\partial}{\partial x_j}\left(K_j\frac{\partial \mathbf{U}}{\partial x_j}\right), \quad (3.1)$$

$$\frac{\partial \rho}{\partial t} + (\mathbf{U}\nabla)\rho = \frac{\partial}{\partial x_j}\left(K_{\rho j}\frac{\partial \rho}{\partial x_j}\right), \quad (3.2)$$

$$(\nabla \mathbf{U}) = 0, \quad (3.3)$$

$$\frac{\partial b}{\partial t} + (\mathbf{U}\nabla)b = \frac{\partial}{\partial x_j}\left(K_{bj}\frac{\partial b}{\partial x_j}\right) + K_j\left(\frac{\partial U_i}{\partial x_j} + \frac{\partial U_j}{\partial x_i}\right)\frac{\partial U_i}{\partial x_j} + K_{\rho z}\frac{g}{\rho}\frac{\partial \rho}{\partial z} - K_j\frac{c^4 b}{l_j}. \quad (3.4)$$

Here $\mathbf{U}$ is the mean velocity vector, p is pressure, ρ is density, all of which are averaged over the turbulent fluctuations; b is the density of the kinetic energy of turbulence, l_j are the turbulence scales, and c^4 is an empirical constant (Monin and Yaglom 1971). According to simple closure hypothesis,

$$K_j = l_j\sqrt{b}, \quad K_{\rho j} = K_j\kappa_\rho, \quad K_{bj} = K_j\kappa_b. \quad (3.5)$$

For the ocean the following empirical values of these constants are typical: $\kappa_\rho = 0.1$ and $\kappa_b = 0.7$.

In the absence of IW this system may be used to define a stationary distribution of flow velocity and turbulent energy over depth (Rodi 1987). Here, we consider these profiles as given and, even if not strictly stationary, then at least changing slowly enough with temporal scales much larger than the ones of the IW. The detailed theoretical analysis of the IW damping by small-scale turbulence has been presented by Ostrovsky and Zaborskikh (1996), where the damping rates have been calculated for IW of different modes in a more complicated situation of shear flow with turbulence. Here, we use their analytical results to estimate the damping rates and coefficients in our experiment. As mentioned, here the turbulence is supposed to be isotropic; that is, the turbulence scales are taken to be the same in all three directions and constant,[2] and the mean flow is absent. The solution of the system of equations (3.1)–(3.5) was sought by the perturbation method, with oscillating components caused by the small-amplitude internal wave:

$$(u', w', \rho', b') = [u(z), w(z), \rho(z), b(z)] \times \exp[i(kx - \omega t)]. \quad (3.6)$$

It is supposed that the IW damping is small at the wavelength scale.

Referring to the paper by Ostrovsky and Zaborskikh (1994), we give only final formulae for calculations of IW damping rate:

[2] The question of the characteristic length scale of turbulence is complicated enough (see Barenblatt 1978 or experimental data by Drayton 1994). In our case it was natural to take l of the order of the perforation scale ($l = 3$ cm): most of relevant works suggest it; moreover, we have indirectly verified it by measuring the turbulence distribution in a nonstratified fluid and calculating the corresponding value of which was proved to be of about 2 cm. For a free small-scale turbulence this value can be supposed constant, at least within the limits of the experimental data dispersion.

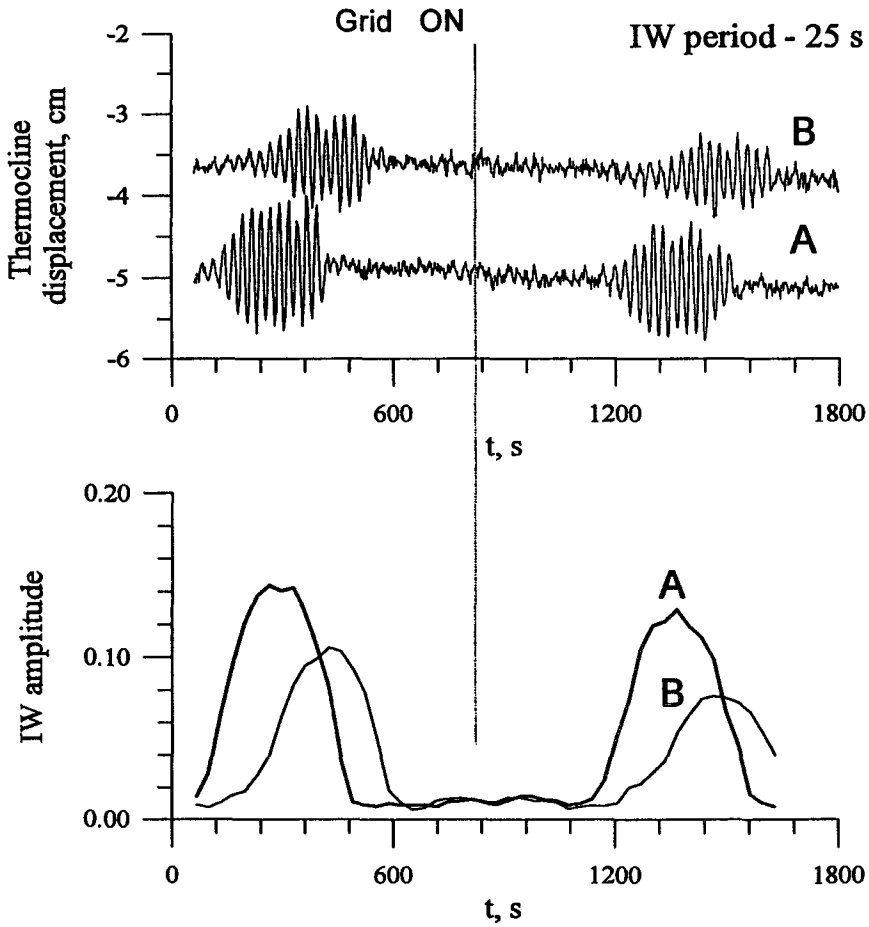

FIG. 6. Experiment with IW trains. The lower plot represents the envelopes of IW. Notations are the same as in Fig. 5.

$$-i\omega_1 = \left(2\int_{-H}^{0} N^2 w_0^2 dz\right)\left\{k^2 \int_{-H}^{0} K_{\rho x} N^2 w_0^2 dz + \frac{\omega_0^2}{k^2}\int_{-H}^{0} w_0\left[\frac{d^2}{dz^2}\left(K_z \frac{d^2 w_0}{dz^2}\right) + K_z k^4 w_0 - 2k^2 \frac{d}{dz}\left(K_z \frac{dw_0}{dz}\right)\right]dz\right\}, \quad (3.7)$$

where $w_0(z)$—vertical velocity amplitude of IW and $\omega_0(k)$ is given by the dispersion law found from the solution of the nondissipative boundary problem for the equation

$$\frac{d^2 w_0}{dz^2} + k^2\left(\frac{N^2}{\omega_0^2} - 1\right)w_0 = 0 \quad (3.8)$$

with boundary conditions

$$w_0 = 0, \quad z = -H, 0. \quad (3.9)$$

The computations have been performed under conditions of the experiment; namely, the $N(z)$ profile and spatial distribution $b(x, z)$ shown in Figs. 2 and 4 have been used. Moreover, Eqs. (3.6)–(3.8) do not take into account the variation of profiles $N(z)$ and $b(z)$ along the tank, which may cause the underestimate of the decay coefficient of IW. Indeed, the first profile depends weakly on the horizontal coordinate, but the turbulence is produced by the grid that is narrow in the x direction, resulting in a pronounced localization of turbulent energy around the grid (see Fig. 4). To consider the x dependence of vertical profiles of $b(z)$ we approximated this spatial distribution by six various 10-cm thick vertical layers with different profiles $b(z)$. The resulting damping rate (the decrement) has been calculated as an average of the decrements $\omega_1(k)$ within each layer.

The results of the calculations are presented in Fig. 8. Here, the functions $\omega_1(k)$ are given for (1) $b = b(x, z)$ as shown in Fig. 4, and (2) $b = 0.0025$ cm^2 s^{-2} = const. For the latter case it is evident that at large k, $\omega_1 \propto k^2$, [as may be easily estimated directly from (9)

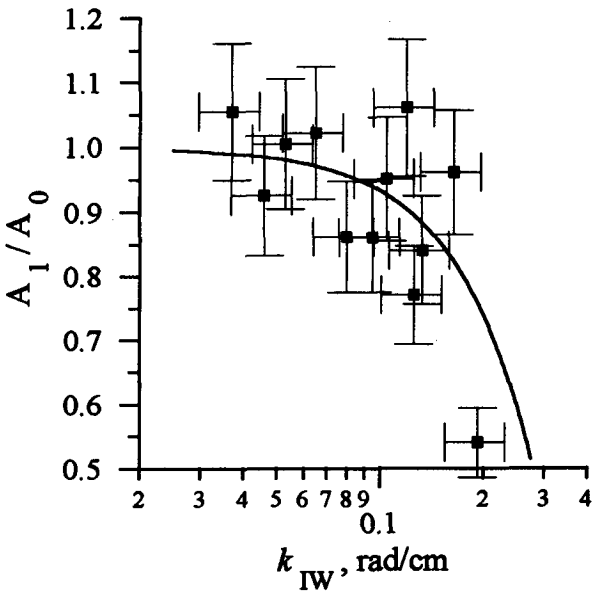

FIG. 7. IW damping (A_1/A_0 ratio) as a function of the wavenumber. The solid curve represents theoretical calculations; squares correspond to experimental data. Vertical and horizontal bars mark the possible experimental errors.

for the case N = const and b = const]. In the first case such an asymptotic is not so obvious: with the change of k the mode structure is also changed. The damping rate of short IW is smaller in this case because the wave energy is concentrated mainly in the narrow vicinity of the sharp thermocline, where the turbulence level is smaller than above (see Fig. 2). Hence, it should be noted that the account of homogeneous turbulence level above the thermocline (which is often used in theoretical papers) can result in considerable overestimation of decay rates of short IW.

The damping rate can be evaluated from the characteristic length L of the turbulent layer and the total decrease of the IW amplitude after passing the layer

$$\frac{A_1}{A_0} = \exp\left(\frac{\omega_1 L}{v_g}\right), \qquad (3.10)$$

where A_0 and A_1 are the IW amplitudes before and after passing through the turbulent region, respectively, $v_g = d\omega_0/dk$ is the wave group velocity; hence L/v_g is a characteristic time when the IW loses its energy at the distance L. The values of A_1/A_0 corresponding to the decay rate w_1 given by curve (1) in Fig. 8 are calculated according to (3.10) and plotted in Fig. 7 together with experimental data. A good quantitative agreement can be observed, thus confirming, at least in the limits of the experimental errors, the validity of the semiempirical model with a constant turbulent scale adopted here.

4. Conclusions

In this paper the results of an experimental study of IW damping by a small-scale turbulence are presented together with estimates based on the semiempirical theory. Although the problem of the interaction between IW and turbulence has been extensively discussed before, this study is probably the first one with quantitative measurements of IW damping for conditions modeling those occurring in reality: thermocline-type stratification and spatial distribution of turbulent energy caused by the wind stress and/or surface wave breaking. It was shown that IW may decay significantly, even passing through a relatively narrow (about a wavelength long) turbulent region with a moderate value of turbulent energy, and the dependence of the damping rate on the wavenumber has been measured. It seems remarkable that a rough theoretical model developed on the basis of a semiempirical theory of turbulence has shown good quantitative agreement with experimental data, even though the turbulent Reynolds numbers were moderate (typically within the interval 500 to 2000), and the turbulence could not be considered as fully developed. It seems that such a loose restriction is characteristic of "free" turbulence, rather than that of boundary-layer flows.

At the same time, the further development of both measurement setup and the theoretical model may give much more information. In particular, accounting for shear flow and the influence of turbulent mixing on the stratification parameters will permit expanding the range to real situations that can be modeled in the tank and reducing the experimental uncertainties. However, taking into account that any experimental measurements involving simultaneously internal waves and turbulence in a stratified fluid are very complicated, we

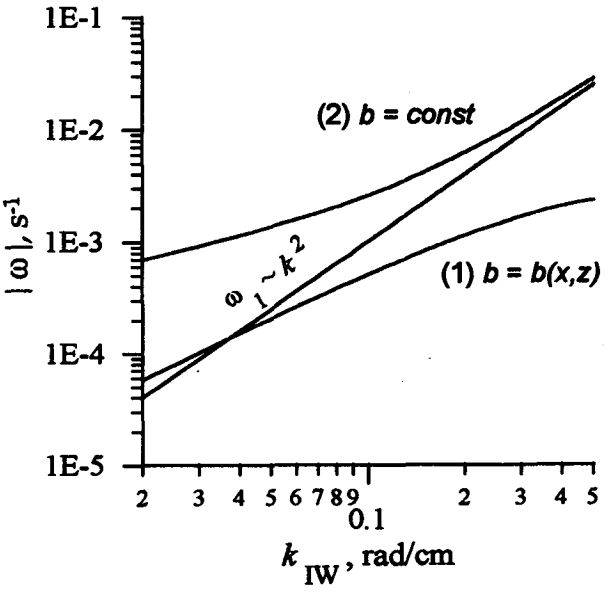

FIG. 8. IW decay rate computed for $b = b(x, z)$ (as measured in experiment) (1) and uniform turbulence distribution (2). The straight line represents the law $\omega \propto k^2$.

believe that the results presented above may be of some significance in understanding the processes in the upper ocean.

Acknowledgments. Support from the joint NOAA/DOD Advanced Sensor Applications Program is gratefully acknowledged.

REFERENCES

Arabadzhi, V. V., S. J. Baranov, S. D. Bogatyrev, V. A. Brailovskaya, V. I. Kazakov, V. R. Kogan, Yu. A. Stepanyants, and V. I. Talanov, 1984: Laboratory basin for the modeling of wave motions in the stratified ocean. *Methods of Hydrophysical Research,* A. V. Gaponov-Grekhov and S. A. Khristianovich, Eds., IAP Acad. Sci. USSR, 5–28.

Barenblatt, G. I., 1978: Strong interaction of gravity waves and turbulence. *Izv. Acad. Sci. USSR, Atmos. Oceanic Phys.,* **13,** 581–583.

Britter, R. E., 1983: Laboratory experiments on turbulence in density-stratified fluids. *Eighth Symp. on Turbulence and Diffusion,* San Diego, CA (unpublished invited paper).

Gargett, A. E., 1984: Internal waves and mixing in the ocean: Observations and speculations. *Internal Gravity Waves and Small-Scale Turbulence, Proc. "Aha Huliko," a Havaian Winter Workshop,* P. Muller and R. Pujalet, Eds., Hawaii Inst. of Geophys., 77–88.

Hopfinger, E. J., 1987: Turbulence in stratified fluids: A review. *J. Geophys. Res.,* **92,** 5287–5303.

Ivanov, A. V., L. A. Ostrovsky, I. A. Soustova, and L. S. Tsimring, 1983: Interaction of internal waves and turbulence in the ocean. *Dyn. Atmos. Oceans,* **7,** 221–232.

Kantha, L. H., 1980: Laboratory experiments on attenuation of internal waves by turbulence in the mixed layer. *Trans. Second Int. Symp. on Stratified Flows,* Irondheim, Norway, IAHB, 731–741.

LeBlond, P. H., 1966: On the damping of internal gravity waves in a continuously stratified ocean. *J. Fluid Mech.,* **25,** 121–142.

Matusov, P. A., L. A. Ostrovsky, and L. S. Tsimring, 1989: Amplification of small-scale turbulence by internal waves. *Dokl. Akad. Nauk SSSR,* **307,** 979–984.

Miropolsky, Y. Z., 1981: *Dynamics of Internal Gravity Waves in the Ocean.* Gidrometeoizdat, 302 pp.

Monin, A. S., and A. M. Yaglom, 1971: *Statistical Fluid Mechanics; Mechanics of Turbulence,* The MIT Press, 769 pp.

——, and R. V. Ozmidov, 1985: *Turbulence in the Ocean.* Dodrecht-Cluver, 247 pp.

Ostrovsky, L. A., and I. A. Soustova, 1979: Upper mixed layer of the ocean as a sink of internal wave energy. *Okeanologia,* **19,** 973–981.

——, and D. V. Zaborskikh, 1996: Damping of internal gravity waves by a small-scale turbulence. *J. Phys. Oceanogr.,* **26,** 388–397.

Phillips, O. M., 1980: *Dynamics of the Upper Ocean.* 2d ed. Cambridge University Press, 336 pp.

Rodi, W., 1987: Examples of calculation methods for flows and mixing in stratified fluids. *J. Geophys. Res.,* **92,** 5305–5328.

Thorpe, S. A., 1973: Turbulence in stably stratified fluids: A review of laboratory experiments. *Bound.-Layer Meteor.,* **5,** 95–119.

Weinstock, J., 1987: The turbulence field generated by a linear gravity wave. *J. Atmos. Sci.,* **44,** 410–420.

Woods, J. D., 1968: Wave-induced shear instability in the summer thermocline. *J. Fluid Mech.,* **32,** 791–800.